Simulation of photoelectric X-ray polarimetry and reconstruction of the photoelectron azimuthal angle [*]

WANG Shuo(王烁)[1,2]   JI Jian-Feng(季建峰)[1,2;1)]   HAN Dong(韩冬)[1,2]   FENG Hua(冯骅)[1,2]

[1] Department of Engineering Physics, Tsinghua University, Beijing 100084, China
[2] Key Laboratory of Particle and Radiation Imaging (Tsinghua University), Ministry of Education, Beijing 100084, China

Abstract: Sensitive X-ray polarimetry in the keV energy range can be achieved by measuring the azimuthal angle distribution of emitted electrons after the photoelectric absorption of X-rays in a micropattern gas detector. However, the initial direction of the electron is not readily measurable due to the randomization of its motion during energy loss. By using the Geant4, Maxwell and Garfield packages, we simulated the detected electron tracks following photoelectric absorption, electron drift and diffusion in the gas, and proposed a technique capable of reconstructing the initial direction of the emitted photoelectron. The technique allows us to measure the angular modulation of flux predicted for a polarized X-ray beam. We calculated the modulation factors in 2–10 keV with a gas mixture of neon and CO_2, and discussed how electron diffusion along the drift will dilute the track and suppress the modulation. These results are useful for the design of the X-ray polarimeter.

Key words: X-ray, polarimetry, micropattern gas detector

PACS: 95.75.Hi   **DOI:** 10.1088/1674-1137/37/3/036002

1   Introduction

X-ray polarimetry is of great interest in high energy astrophysics. It has been predicted that significant polarization can be detected from bright X-ray sources such as accreting black holes, pulsars, and supernova remnants, and the degree and position angle of the polarization would place useful constraints on the emission mechanism of these objects [1]. Over the past decade, a new, sensitive means for X-ray polarimetry based on the photoelectric effect has been proposed and successfully tested in the laboratory [2, 3]. The K-shell cross section of the photoelectric effect [4, 5] can be written as

$$\frac{\mathrm{d}\sigma}{\mathrm{d}\Omega}=r_0^2\frac{Z^5}{137^4}\left(\frac{m_0c^2}{h\nu}\right)^{7/2}\frac{4\sqrt{2}\sin^2\theta\cos^2\phi}{(1-\beta\cos\theta)^4}, \qquad (1)$$

where r_0, m_0, β, Z, and $h\nu$ are, respectively, the classical electron radius, electron mass, electron velocity, atomic number, and photon energy. θ is the polar angle and ϕ is the azimuthal angle of the emitted photoelectron. On the plane perpendicular to the incident X-ray, the projected position angle $(=\phi)$ of the emitted photoelectron followed by absorption of the X-ray photon has a distribution $\propto\cos^2\phi$, where $\phi=0$ indicates the direction of the electric vector of the X-ray electromagnetic wave. Thus, one can measure the linear polarization of the X-ray beam by imaging the track of each photoelectron on the detection plane. In the keV energy range, the length of the track is on the order of millimeter. Micropattern gas detectors like gas electron multipliers (GEMs) with a position accuracy of around 100 μm are capable of such an application. In cases where a large detecting area and/or high quantum efficiency is needed, one dimensional strips with a timing projection readout have advantages over the traditional two dimensional image readout [6]. This technique is also proposed for X-ray polarimetry on future space astronomical missions in China such as the X-ray timing and polarization satellite.

One of the key issues for such a technique is that, due to the small mass of an electron, it does not leave a straight track during energy loss in the gas detector. An algorithm is needed to reconstruct the initial azimuthal angle of the electron from a randomized track. The only way to address this problem is to use simulations where the exact azimuthal angle is known. To do so, one needs to trace both the electromagnetic interactions in the detector and the drift and multiplication of electrons toward the multiplier and the readout. In this paper, we reported the construction of simulation packages, including Geant4 [7], Maxwell, and Garfield, and propose a method that allows us to restore the initial photoelectron azimuthal angle.

2   Detector configuration and simulation packages

The detecting gas is a mixture of 70% neon and 30% CO_2 at total pressure of half atmosphere. This mixture is optimized for X-ray polarimetry in the 2–10 keV energy range. A schematic drawing of the detector is shown in Fig. 1, including a drift plane, a GEM foil of 50 μm thick and 140 μm pitch of holes, and strip readout of 140 μm pitch. X-rays incident from the side of the detector, along the $-Z$ direction, between the drift and GEM. A 2-D image of energy deposits by secondary electrons on the plane perpendicular to the X-ray direction will be taken. The strips provide the Y coordinates and the timing information gives the X coordinates.
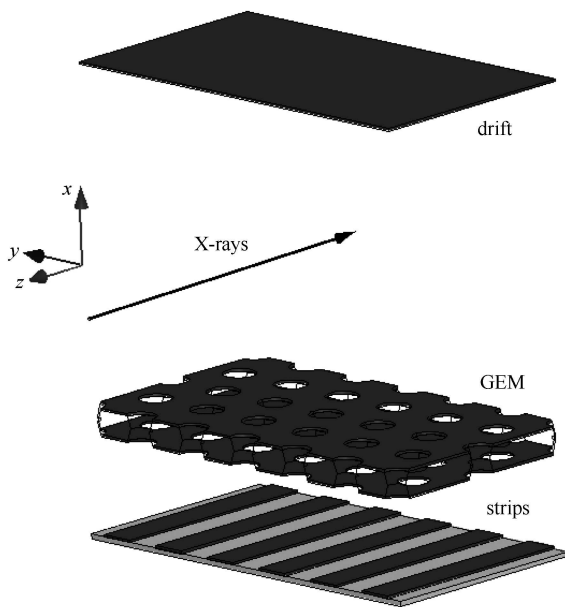

Fig. 1.   Schematic drawing of the detector, not to scale.

The GEANT4 package is used to simulate the interaction of X-rays with the gas. The major interaction in this energy range is the photoelectric effect. To enable the cross section with polarization, we adopted the model G4Livermore Polarized Photo Electric Model in GEANT4. The K-shell electron binding energy of neon is 870.2 eV. Following the photoelectric absorption, an electron (photoelectron) is emitted with a kinetic energy equal to the X-ray energy minus the binding energy. The atom will then emit either an Auger electron or a fluorescent photon (most likely due to the transition from L to K shell). The electrons will then lose energy in the gas through ionization and excitation and leave behind a track consisting of electrons and ions. As the Auger electron is much less energetic than the photoelectron, it will stop very close (less than the readout can resolve) to the X-ray interaction point while the photoelectron will travel to a distance of about one millimeter away from the interaction point. Fig. 2 shows the energy deposits projected on the XY plane by absorbing a 6 keV X-ray.
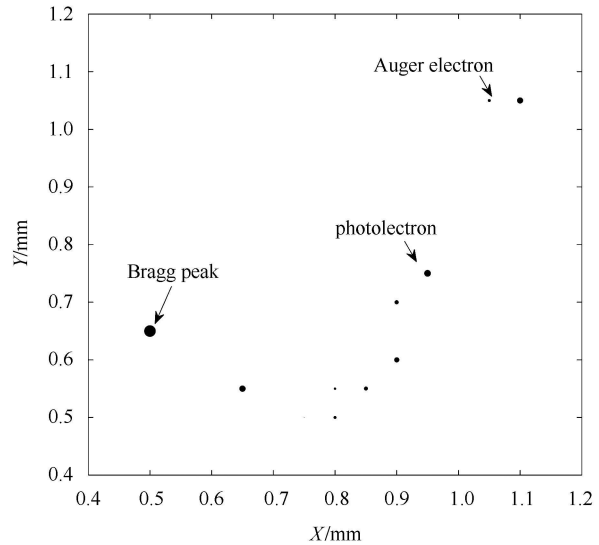

Fig. 2.   The energy deposits projected on the XY plane following the absorption of a 6 keV X-ray in the gas, simulated with Geant4. The Auger electron stops near the interaction point, while the photoelectron travels away.

Due to the presence of the drift field, the electrons created by ionization will move toward the GEM, be multiplied, and collected by strips beneath the GEM. The drift and multiplication of the electrons are simulated in Garfield with the electric field imported from Maxwell. The most important parameters in this process are the drift velocity, which affects the scale on the X direction, and the electron diffusion, which affects the resolution of the image. The drift velocity, transversal and vertical diffusions are shown in Fig. 3. The drift velocity v_d, on the order of $\sim$cm/μs, varies with the drift field. To have symmetric scales on both X and Y direction, the sampling timescale is set to $\Delta t = 140$ μm/v_d. The preamplifier has a discharge time scale much longer than Δt, suggesting that the detected signal waveform reflects accumulated electrons on each strip at a given time, see Fig. 4. In the simulation, the gain of the GEM is adjusted to be 2000. A noise of 500 e^- rms from the preamplifier is added into the output waveform. The drift distance is set to have a transversal diffusion of 100 μm. Then, the collected electrons during each time step, Δt, is the difference of the waveform, see Fig. 5 for images.
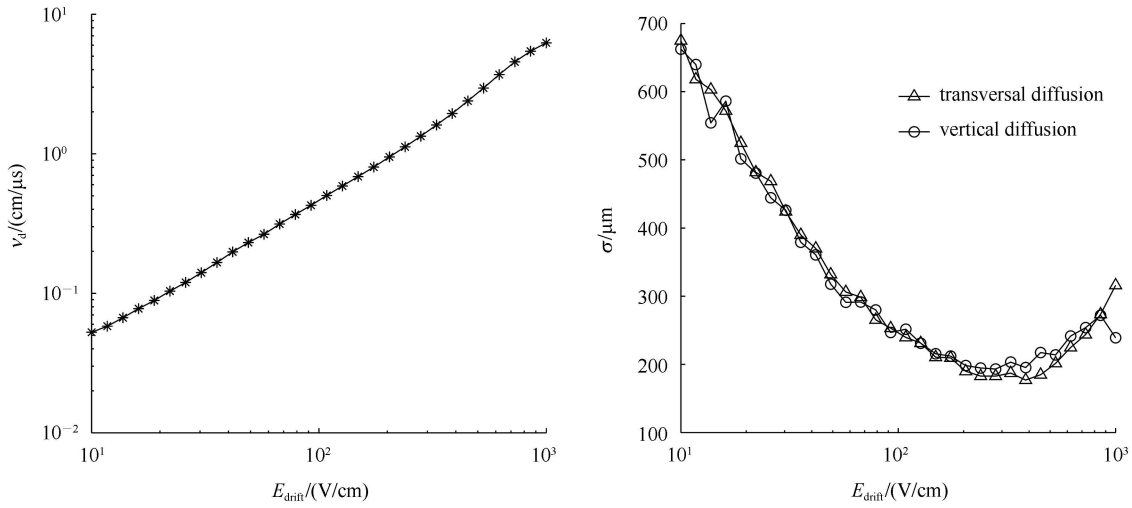
Fig. 3.   The electron drift velocity v_d and diffusion σ after 1 cm drift versus the drift field $E_{\rm drift}$ in a gas mixture of 70% neon and 30% CO_2 at a pressure of half atmosphere.
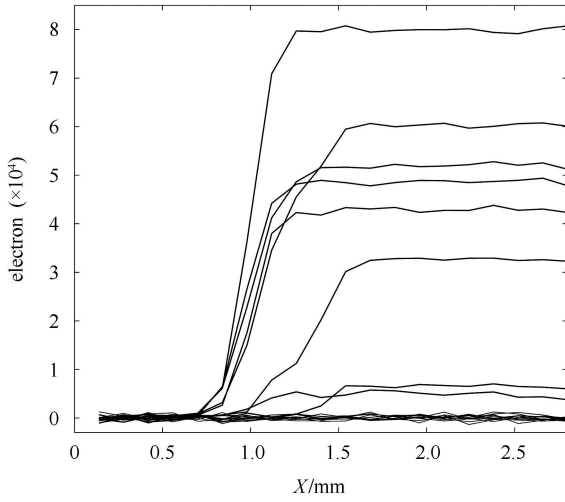

Fig. 4.   The simulated waveform on each strip. The X position is converted from the drift time, $\Delta X = \Delta T v_d$.

3   Reconstruction of the azmuthal angle

One can fit the azimuthal angle distribution with the following function,

$$A + B\cos^2(\phi - \phi_0), \qquad (2)$$

where A, B, and ϕ_0 are the parameters that account for the nonpolarized component, the polarized component, and the polarization position angle, respectively. The degree of modulation is defined as

$$\mu = \frac{C_{\rm Max} - C_{\rm Min}}{C_{\rm Max} + C_{\rm Min}} = \frac{B}{2A+B}, \qquad (3)$$

where $C_{\rm Max}$ and $C_{\rm Min}$ are the maximum and minimum values of the modulation curve. The degree of modula-

tion of a fully polarized beam is called μ_{100}. The degree of polarization is thus defined as $\Pi = \mu/\mu_{100}$.

Due to the Coulomb scattering by the nucleus, the degree of modulation is not 100%. The randomization of the electron motion may increase the uncertainty of measuring the azimuthal angle of the photoelectron. This will further suppress the modulation factor μ_{100} if no proper algorithm is invoked to reconstruct the initial azimuthal angle.

It is of great importance to build an instrument with a large modulation factor (μ_{100}), which is directly related to the sensitivity. The sensitivity of the polarimeter is defined as the minimum detectable modulation (MDP). The MDP at 99% confidence level can be written as [8]

$$\text{MDP} = \frac{4.29}{\mu_{100}S}\sqrt{\frac{S+B}{T}}, \qquad (4)$$

where S and B are the source and background count rate, respectively, T is the observing time. As one can see, the modulation factor is one of the most important factors that determines the sensitivity. In cases of observing bright objects, i.e., $S \gg B$, then $\text{MDP} \propto 1/(\mu_{100}\sqrt{S})$ gives an observing time. This means the modulation factor μ_{100} is even more effective than the collecting area to increase the sensitivity.

A straightforward way to obtain the azimuthal angle, based on the detected electron track, is to calculate the major orientation (principal axis) of the track. The barycentric point of the track is

$$\bar{x} = M_{10}/M_{00}, \qquad (5)$$

$$\bar{y} = M_{01}/M_{00}, \qquad (6)$$

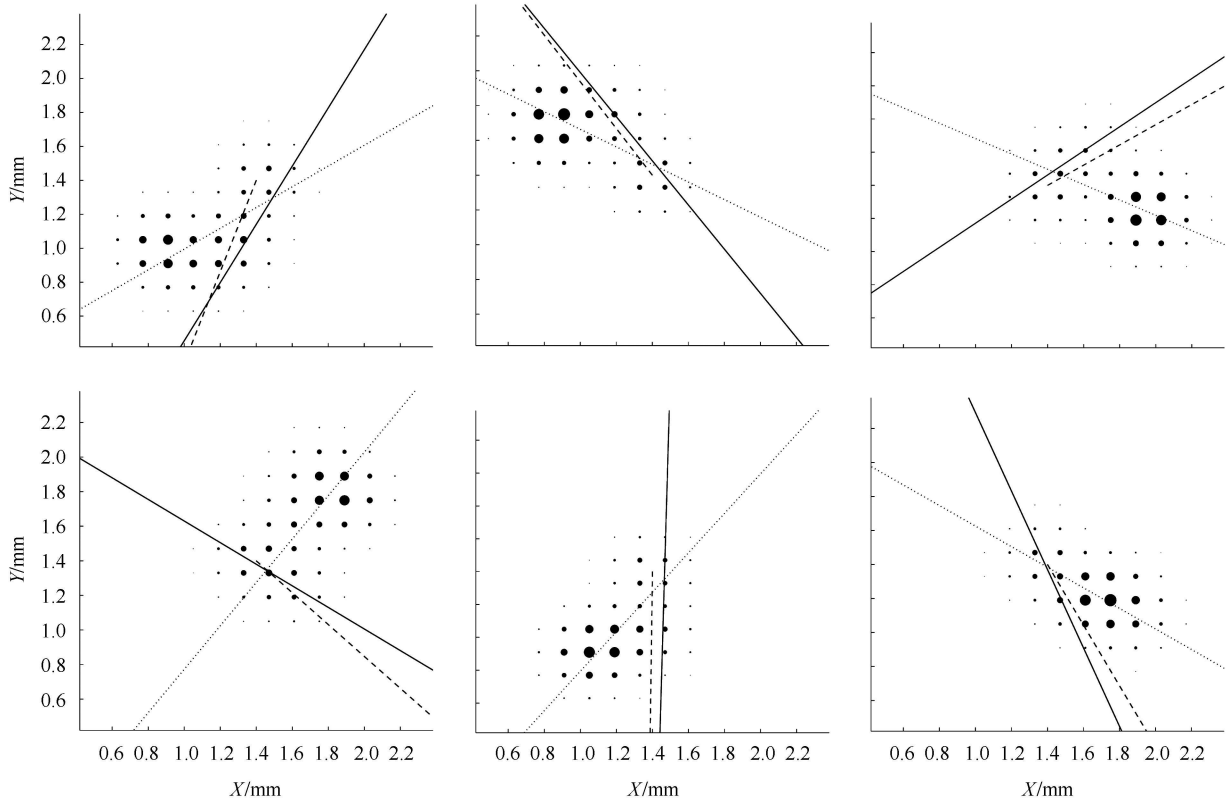where $M_{\rm pq} = \sum_{x,y} x^{\rm p} y^{\rm q} f(x,y)$ standing for the moment of

Fig. 5.　The simulated tracks of detecting 6 keV X-rays. The dashed line indicates the initial direction of the emitted photoelectron. The dotted line represents the reconstructed direction by calculating the orientation of the overall track. The solid line indicates the reconstructed direction using the algorithm that we proposed.
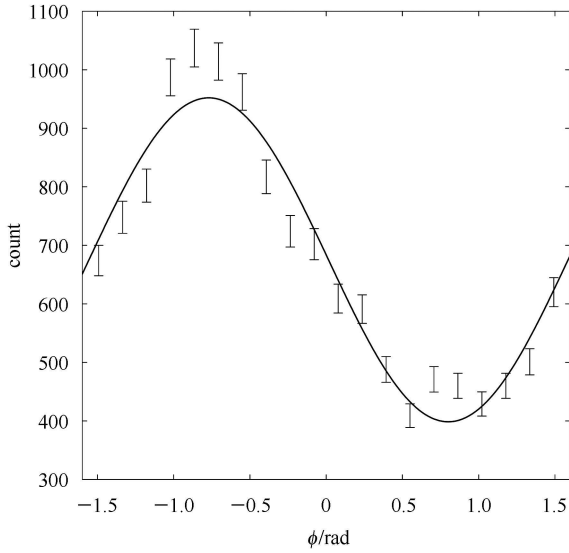

Fig. 6.　The distribution of reconstructed azimuthal angle for 6 keV X-rays.

the image $f(x,y)$ with the order of (p, q). The orientation of the track can be written as

$$\alpha=\frac{1}{2}\tan^{-1}\left(\frac{2\mu_{11}}{\mu_{20}-\mu_{02}}\right), \tag{7}$$

where

$$\mu_{11} = M_{11}/M_{00}-\bar{x}\bar{y}, \tag{8}$$

$$\mu_{20} = M_{20}/M_{00}-\bar{x}^2, \tag{9}$$

$$\mu_{02} = M_{02}/M_{00}-\bar{y}^2. \tag{10}$$

However, as shown in Fig. 5, the orientation calculated in such a way (dotted line) is not consistent with the true azimuthal angle (dashed line) at all. As we have discussed above, the X-ray interaction point usually has an energy deposit of the auger electron, or zero in case where a fluorescent photon is emitted, whereas, around the ending point of the photoelectron, most of the energies are deposited (the Bragg peak). This physical constraint helps us to find the interaction point of the photoelectric absorption, which can be identified with the third order moments of the image [4]. Then, if we re-calculate the orientation using pixels around the interaction point, the derived orientation (solid line) is very consistent with the azimuthal angle of the photoelectron.

With the algorithm above, we plotted the modulation curve for 6 keV X-rays in Fig. 6 and calculated the degree of modulation of nearly 0.4. The modulation factor is nearly zero at 2 keV, due to the small energy of

the photoelectron which cannot be resolved by the readout. The modulation factor will increase with increasing the X-ray energy (Fig. 7). The modulation factor peaks around 0.5, close to the value of about 0.7 calculated by counting the true azimuthal angle, which is not unit due to the fact that the photoelectron will be scattered by
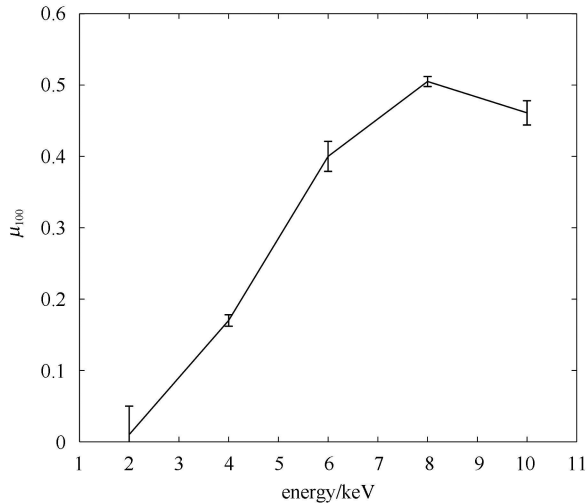

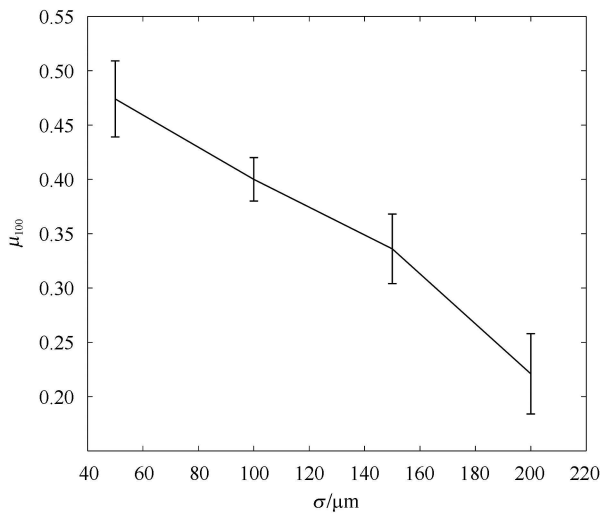Fig. 7.   Modulation factor μ_{100} versus X-ray energy.

Fig. 8.   Modulation factor μ_{100} at 6 keV versus transversal diffusion σ.

the nucleus when it is emitted. The diffusion, readout noise and resolution will further decrease the detected modulation factor.

Due to transversal diffusion, the track image will be smoothed along drift. This fuzzy image will prevent us from precisely reconstructing the azimuthal angle. As shown in Fig. 8, the modulation factor at 6 keV decreases from about 0.5 to nearly 0.2 if the diffusion changes from 50 μm to 200 μm.

4   Conclusions and discussions

We have built up software packages capable of simulating the physical processes in a photoelectric X-ray polarimeter. This allows us to optimize the instrument design and test the algorithm to restore the photoelectron azimuthal angle and thus the modulation factor.

As shown above, the modulation factor is one of the most important parameters of a polarimeter and determines the sensitivity directly. For photoelectric X-ray polarimeters, the way to maximize the modulation factor is to precisely measure the azimuthal angle of the emitted photoelectron. Based on the physics in the detector, we find that this can be done by identification of the interaction point, where less energy is deposited than at the other end of the track, which is the Bragg peak. With this technique, the modulation factor can be restored to about 80% of its intrinsic value; electron diffusion along drift prevents us from a complete restoration.

From the simulations we learned that for even longer drift distances, the electron diffusion will dilute the track and decrease the modulation factor. The diffusion (σ) scales with the square root of the drift distance (D), i.e. $\sigma \propto \sqrt{D}$. From Fig. 3, which shows the diffusion after 1 cm drift, $\sigma = 200$ μm corresponds to a drift distance of about 1 cm. Therefore, we conclude that for any polarimeter that requires a drift distance comparable to or longer than 1 cm, the diffusion cannot be neglected and will greatly decrease the accuracy of the measurement and the sensitivity of the instrument. In these cases, negative ions such as nitromethane will be needed to suppress the electron diffusion [9].

References

1 Kallman T. Adv. Space Res., 2004, **34**: 2673–2677
2 Costa E, Soffitta P, Bellazzini R et al. Nature, 2001, **411**: 662–665
3 Black J K, Deines-Jones P, Ready, S E et al. Nucl. Instrum. Methods A, 2003, **513**: 639–643
4 Bellazzini R, Angelini F, Baldini L et al. Proc. SPIE, 2003, **4843**: 383–393
5 Depaola G O, Longo F. Nucl. Instum. Methods A, 2006, **566**: 590–597
6 Black J K, Baker R G, Deines-Jones P et al. Nucl. Instum. Methods A, 2007, **581**: 755–760
7 Agostinelli S, Allisonas J, Amako K et al. Nucl. Instum. Methods A, 2003, **506**: 250–303
8 Novick R. Planets, Stars and Nebulae: Studied with Photopolarimetry. Gehrels T. Tucson: University of Arizona Press, 1974. 262
9 Prieskorn Z R, Hill J E, Kaaret, P E et al. IEEE Trans. Nucl. Sci., 2011, **58**: 2055–2059